

Supporting Information

Intense electrochemiluminescence from organic microcrystals accelerated H₂O₂-free luminol system for microRNA detection

Li Wang, Ming-Hui Jiang, Ya-Qin Chai, Ruo Yuan and Ying Zhuo*

Chongqing Engineering Laboratory of Nanomaterials & Sensor Technologies, College of

Chemistry and Chemical Engineering, Southwest University,

Chongqing 400715, China

*Corresponding author. **Tel:** +86-23-68253172; **Fax:** +86-23-68253172.

E-mail address: yingzhuo@swu.edu.cn. (Y. Zhuo).

1. Reagents and Material

9,10-Diphenylanthracene (DPA) and the adenosine triphosphate (ATP) were gained from J&K Chemical Technology (Beijing, China). Luminol (98%), gold chloride tetrahydrate ($\text{HAuCl}_4 \cdot 4\text{H}_2\text{O}$, 99%), $\text{K}_4\text{Fe}(\text{CN})_6$, poly-(diallyldimethylammonium chloride) (PDDA), hexanethiol (HT, 96%), 1-(3-(Dimethylamino)propyl)-3-ethylcarbodiimide hydrochloride (EDC), N-hydroxy succinimide (NHS), sodium borohydride (NaBH_4), L-ascorbic acid (AA), trisodium citrate ($\text{Na}_3\text{C}_6\text{H}_5\text{O}_7$) and tris (2-carboxyethyl)phosphine hydrochloride (TCEP) were obtained from Sigma-Aldrich (St. Louis, MO, USA). Cetyltrimethylammonium bromide (CTAB), tetrahydrofuran (THF), ethylenediaminetetraacetic acid (EDTA), polyethylene glycol-800 (PEG-800), acetic acid (NaAc), dimethyl sulfoxide (DMSO), p-benzoquinone and ethylene glycol (EG) were all purchased from Kelong Chemical Inc. (Chengdu, China). Dopamine (DA) was received from bide pharmaceutical technology Co. Ltd. (Shanghai, China). Silver nitrate (AgNO_3 , 99.8%) was supplied by Sinopharm Chemical Reagent Co. Ltd. (Shanghai, China). Ferric chloride ($\text{FeCl}_3 \cdot 6\text{H}_2\text{O}$) was brought from Qiangshun Chemical Reagent Co. Ltd. (Shanghai, China). T7 Exonuclease (T7 Exo) was obtained from New England Biolabs (Ipswich, MA).

All the oligonucleotides that appeared in this research process were synthesized at Sangon Biotech Co. Ltd. (Shanghai, China), and the corresponding sequences were displayed in Table 1. The buffers involved in this work were presented as follows. The phosphate buffered saline (PBS, 0.1 M, pH 7.4) was comprised of 0.1 M Na_2HPO_4 , 0.1 M KH_2PO_4 , and 0.1 M KCl. $1 \times$ NE Buffer (pH 7.9) was prepared with 50 mM KAc,

20 mM Tris-Ac, 10 mM Mg(Ac)₂ and 1 mM DTT. 1 × TE buffer (pH 8.0) containing 10 mM Tris-HCl and 1.0 mM EDTA was used to dissolve and store all oligonucleotides. The DNA hybridization buffer (HB, pH 7.4) was composed of 10 mM Tris-HCl, 1.0 mM EDTA and 1.0 M NaCl. Ultrapure water was used throughout the experiment, which derived from Milli-Q water purification system with an electric resistance of 18.2 MΩ.

Table S1. The Sequences of Oligonucleotides Used in This Work

name	Sequences (5' → 3')
S0	5'-GCG AAT GAC TCG TAC CTT CCT CCG CAA TAC TCC CCC-3'
S1	5'-TCG ACT ATC AGA CTG ATC ATT CGC-3'
S2	5'-SH-(CH ₂) ₆ -CGT ACT ATC AGG CAA GCT ACT TAC CTG GGG GAG TAT TGC GGA GGA AGG TTC AAC ATC AGT CTG ATA GTA CG-3'
S3	5'-GGG GGA GTA TTG CGG AGG AAG GTA CGA GTC AAA GCG- (CH ₂) ₆ -SH-3'
S4	5'-COOH-GCG AAT GAC TCG TAC CTT CCT-3'
Micro-21	5'-UAG CUU AUC AGA CUG AUG UUG A-3'

2. Apparatus

The ECL signals and cyclic voltammetric (CV) curves were recorded via a model MPI-E multifunctional analyzer (Xi'An Remax Electronic Science & Technology Co. Ltd., Xi'An, China) and a CHI 660C electrochemical work station (Shanghai Chenhua Instruments, China), respectively. In the above test process, a traditional three-electrode system including glassy carbon electrode (GCE) as working electrode, platinum wire as counter electrode, and Ag/AgCl electrode (with saturated KCl) as reference electrode

was used. The scanning electron microscopy (SEM, S-4800, Hitachi, Tokyo, Japan) was utilized to characterize the morphologies and sizes of different nanomaterials. The ECL spectra were acquired on a CHI 760E combined with a Newton EMCCD spectroscopy detector (Andor Co, Tokyo, Japan).

3. Preparation of the 9,10-diphenylanthracene Microcrystals (DPA MCs)

The DPA MCs were prepared by the surfactant-assisted self-assembly method with minor modifications.¹ First of all, 3 mg of DPA powder was completely dissolved in 3 mL of THF solution. Then, the above solution was rapidly injected into 10 mL of CTAB solution (15 mM) under moderately stirring for 20 min. The final DPA MCs were centrifuged and washed with ultrapure water 4 times, then dispersed in 4 mL of ultrapure water and stored at 4 °C for later use.

4. Synthesis of the Au nanoflowers (Au NFs)

The Au NFs were synthesized according a multistep seeding-based nanotemplating method with subtle adjustments based on previous literature.² First of all, 200 μ L of trisodium citrate solution (25 mM) was mixed with 20.5 mL of H₂AuCl₄ solution (0.25 mM), and 60 μ L of freshly prepared sodium borohydride solution (100 mM) was slowly injected into the above solution with stirring. Then, it was kept in darkness for 2 h until it turned deep red to form a spherical Au nanoseeds. The second step was to synthesize Au pops as growth solution. In brief, 320 μ L of L-ascorbic acid solution (AA, 100 mM) was added dropwise to 47.3 mL of the mixed solution containing

2.7 mM cetyltrimethylammonium bromide (CTAB), 0.43 mM HAuCl₄, 1.1 mM silver nitrate (AgNO₃) under vigorous stirring. Afterwards, 500 μL of as-prepared Au nanoseeds were transferred into the growth solution and kept for another 2 h to obtain the monodispersed Au popcorns. Subsequently, to further synthesize the Au NFs, 320 μL of AA solution (100 mM) was dropwise injected into 47.3 mL of the solution containing 2.7 mM CTAB, 0.43 mM HAuCl₄, 1.1 mM AgNO₃ under intense stirring. After that, 500 μL of as-prepared Au popcorns were slowly added to the above solution and aged for overnight. Finally, the products were collected by centrifugation (8000 rpm, 10 min), redispersed in ultrapure water and stored in a refrigerator at 4 °C.

5. The Synthesis of Au@Fe₃O₄ Nanocomposites

The Au@Fe₃O₄ nanocomposites were synthesized according to the published literature with some adjustment.³ At first, 0.7 g FeCl₃·6H₂O, 0.5g PEG-800 and 1.8g NaAc were dissolved in 20 mL of EG solution and stirred for 30 min, and the mixture was transferred to a 25 mL Teflon reactor with heating at 200 °C for 8 h. Then, the Fe₃O₄ nanoparticle was separated by a magnet and washed with ultrapure water. After drying in the vacuum oven at 80 °C for 12 h, 5.0 mg Fe₃O₄ nanoparticles were dispersed in 5 mL of PDDA aqueous solution (1 wt%) with shaking overnight at room temperature to form positively charged Fe₃O₄ nanoparticles. Following that, 1 mL of negatively charged gold colloidal solution based on the reported method¹ was added into the as-prepared Fe₃O₄ nanoparticles and shaken for 5 h at room temperature to obtain the Au@Fe₃O₄ nanocomposites *Via* electrostatic interaction. Subsequently, the products were collected by magnetic separation and purified by washing with ultrapure

water and ethanol for 3 times, alternately.

6. Preparation of the “Y”-DNA structures (Y-DNA) and Y-DNA/Au@Fe₃O₄ composites

The Y-DNA/Au@Fe₃O₄ composites were obtained as follows. First, S0 (2 μM), S1 (2 μM) and the thiolated S2 (2 μM) were mixed in DNA hybridization buffer (HB) and annealed at 95 °C for 5 min to obtain the Y-DNA. Then, 600 μL of the prepared Y-DNA solution was mixed with 1 mL the suspension of Au@Fe₃O₄ nanocomposites at 4 °C for 12 h on the shaking table to obtain the Y-DNA labeled Au@Fe₃O₄ composites (Y-DNA/Au@Fe₃O₄) through Au-S bond. Eventually, the resultant Y-DNA/Au@Fe₃O₄ composites were collected through magnetic separation and stored at 4 °C for further use.

7. Preparation of the DA-S4 probes

The DA-labeled DNA probes (DA-S4) were prepared as follows. At first, 24 mg EDC and 3.5 mg NHS were added into 200 μL of S4 (5 μM) under softly stirring for 2 h at 4 °C for activating the carboxyl of S4. Then, 300 μL of DA solution (10 mM) was slowly injected into the above mixing solution and stirred overnight for obtaining the DA-S4.

8. The process of target-recycling amplification strategy and RSDR

The target-recycling amplification strategy with the help of ATP was implemented as follows. First, 100 μL of Y-DNA/Au@Fe₃O₄ solution was injected in a centrifuge tube and the supernatant was removed by magnetic separation. Then, 90 μL of target miRNA-21 with various concentrations and 10 μL of ATP (10 μM) were injected into

above centrifuge tube to react at 37 °C for 2 h. Concretely, the miRNA-21 partially hybridized with S2 to release the MT. Then the specific recognition of ATP and S2 (the aptamer of ATP) was accompanied by the release of miRNA-21 to trigger the next cycle. After reaction at 37°C for 1.5 h, the supernatant contained a large number of MT was obtained by magnetic separation. Subsequently, 89 μL of the resultant supernatant, 1 μL of 10000 U/mL T7 Exo and 10 μL of $10 \times$ NE buffer 4 were mixed to form the reaction solution. After that, 10 μL of the reaction solution was dropped on above proposed biosensor (DA-S4/HT/S3/Au NFs/DPA MCs/GCE) to induce the RSDR.

9. Fabrication of the ECL Biosensor

Before the biosensor modification, the glassy carbon electrode (GCE, $\Phi = 4$ mm) was pretreated according to the previous literature.⁴ Afterward, 10 μL of DPA MCs solution was dropped on the clear GCE (DPA MCs/GCE). After drying at room temperature naturally, 5 μL of Au NFs solution was coated on the modified electrode by electrostatic assembly. Afterwards, 10 μL of S3 solution (2 μM) was immobilized on the Au NFs/DPA MCs/GCE at 4 °C for 12 h through Au-S covalent bond. After washing, 10 μL of HT (1.0 mM) was dripped on the resultant electrode (S3/Au NFs/DPA MCs/GCE) for 40 min under room temperature to block nonspecific binding sites. Finally, 10 μL of DA-S4 solution was assembled on the surface of HT/S3/Au NFs/DPA MCs/GCE for 2 h at 37 °C to obtain the biosensor (DA-S4/HT/S3/Au NFs/DPA MCs/GCE). The construction of the biosensor could be proved through cyclic voltammetric (CV) and ECL characterization.

10. ECL Measurement Condition

In the ECL detection process, 2 mL of PBS (pH 7.4) containing 30 μ M luminol was used as the test base solution with the working potential varied from -0.6V~0.6 V, the PMT was 800 V and a scan rate of 0.3 V/s.

11. Polyacrylamide Gel Electrophoresis (PAGE)

The target-recycling amplification process and the enzyme-assisted cycling strand displacement reaction was investigated by PAGE. The prepared samples were analyzed by nondenaturing polyacrylamide gel, and electrophoresis was conducted at 120 V in 1 \times TBE buffer for 120 min. After dyeing by gel green, the electrophoresis image was observed under UV light.

12. ECL and CV Characterization of the ECL Biosensor

The stepwise modification of the biosensor was characterized by ECL and CV. As can be seen in Fig. S1A, an obvious low ECL signal was achieved from the bare GCE in luminol solution (curve *a*), because the low reactivity of luminol/dissolved O₂ system. After the DPA MCs were modified on the electrode surface, the ECL signal enhanced significantly (curve *b*), which was ascribed to the excellent catalytic activity of DPA MCs for dissolved O₂. The ECL signal then was enhanced again after Au NFs modification owing to its excellent conductivity character (curve *c*). After the incubation of the S3, the ECL intensity decreased, which can be attributed to the hindrance of electron transport by DNA (curve *d*). After blocking with HT for 40 min, the ECL signal further declined with the HT impeded the electron transfer (curve *e*). Afterwards, the ECL signal decreased notably when the biosensor was incubated with DA-S4 (curve *f*). The reason was the efficient quenching effect of DA on luminol

luminescence. Ultimately, it should be noted that after the introduction of the MT, the ECL signal achieved recovered (curve *g*), such ECL response can be assigned to that the DA-S4 was replaced by S0 and kept away from the electrode surface.

Besides, Fig. S1B exhibited the CV curves in 5.0 mM $[\text{Fe}(\text{CN})_6]^{3-/4-}$ solution. There were a pair of well-defined redox peaks when bare GCE was detected (curve *a*), which corresponded to the reversible redox reaction of $[\text{Fe}(\text{CN})_6]^{3-/4-}$. And then the peak current value reduced with the modification of DPA MCs (curve *b*), for the poor electrical conductivity of DPA MCs. After the Au NFs were decorated on the above modified electrode, the peak current value increased evidently (curve *c*), because the Au NFs could accelerate the electron transfer as a conductive material. when the S3 (curve *d*) and HT (curve *e*) were successively incubated on the modified electrode, the corresponding CV responses declined in turn for the reason of the DNA and HT impeded. Subsequently, with the DA-S4 incubated on the proposed biosensor, the CV signal decreased notably because of the negatively charged DNA hindered the electron transfer (curve *f*). Subsequently, the CV response made a partial recovery when the reaction solution was coated on the surface of the electrode (curve *g*), because the DA-S4 were released from the electrode surface by RSDR process. Through the above changes, it could be known that the biosensor was successfully constructed.

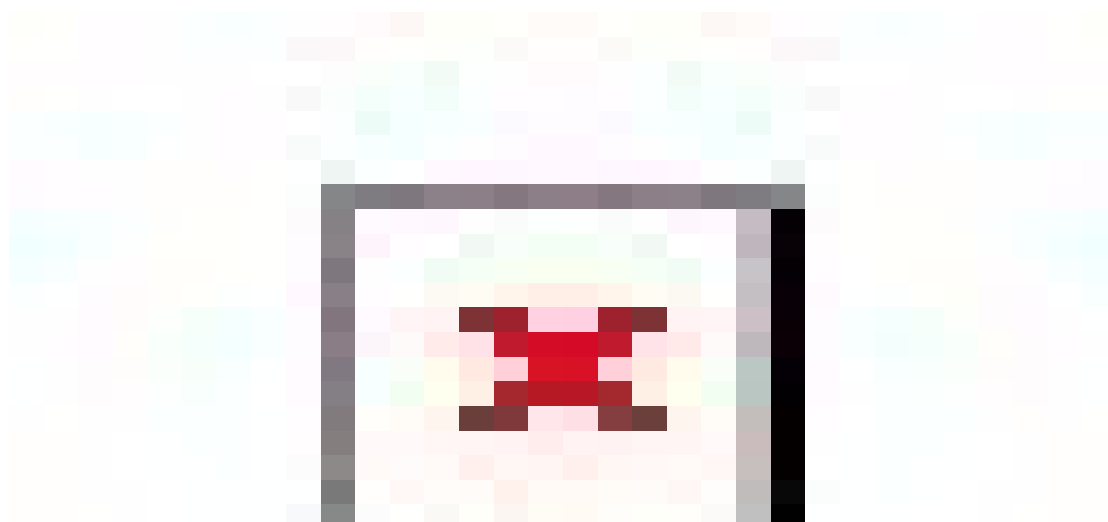


Fig. S1 (A) ECL profiles of the modified electrodes at different states in PBS (pH 7.4) containing 30 μ M luminol and (B) CVs characterizations of the stepwise modified electrodes in PBS (pH 7.4) containing 5.0 mM $[\text{Fe}(\text{CN})_6]^{3-/4-}$ solution: (a) bare GCE, (b) DPA MCs/GCE, (c) Au NFs/DPA MCs/GCE, (d) S3/Au NFs/DPA MCs/GCE, (e) HT/S3/Au NFs/DPA MCs/GCE, (f) S4/HT/S3/Au NFs/DPA MCs/GCE, (g) S0/DA-S4/HT/S3/Au NFs/DPA MCs/GCE.

13. Optimization of the reaction conditions

To achieve an optimal performance of the developed biosensor, the two incubation times of cycle I and cycle II were investigated. As indicated in Fig. S2A, when the incubation time of the miRNA-21 (cycle I) increased from 30 min to 90 min, the ECL intensity kept an upward trend and then reached a platform with the time from 120 min to 180 min. Thus, 90 min was the optimal incubating time for the cycle I. Furthermore, the reaction time of RSDR (cycle II) would directly influence the recovery of ECL signal. As exhibited in Fig. S2B, with the increase of reaction time, the ECL response increased and trended to a platform at 120 min gradually, indicating that 120 min was the optimal reaction time of the RSDR.

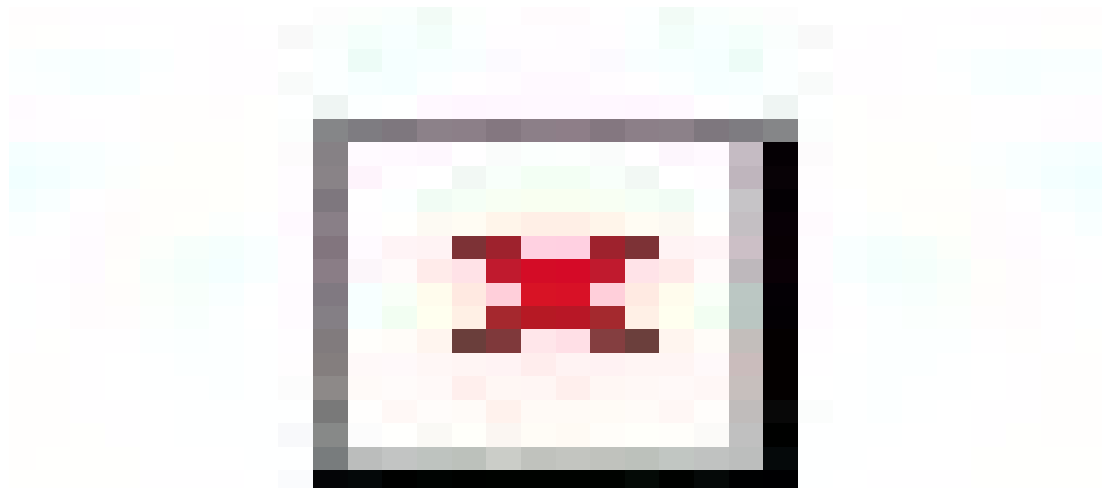


Fig. S2 Experimental optimizations of the proposed biosensor for miRNA-21 detection. (A) The incubation time of miRNA-21 (10 pM, cycle I) and (B) the reaction time of RSDR (cycle II).

14. Application of the MiRNA Biosensor in the Tumor Cells.

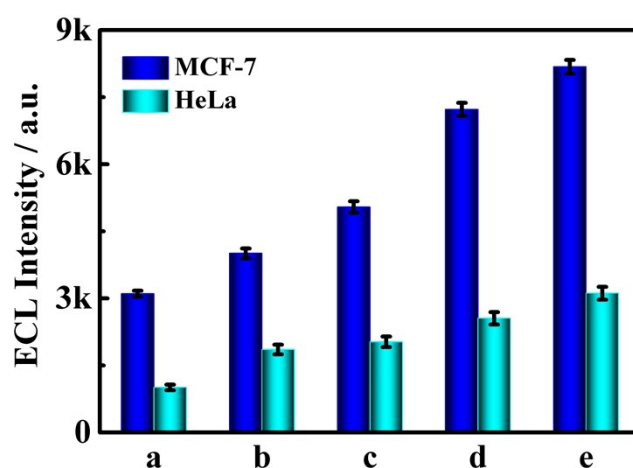


Fig. S3 The real sample analysis of miRNA-21 was performed with different concentrations of different cell lysates: (a) 10 cells, (b) 1×10^2 cells, (c) 1×10^3 cells, (d) 1×10^4 cells and (e) 1×10^5 cells of human cervical cancer cells (HeLa) and human breast cancer cells (MCF-7), respectively.

Table S2 Comparison of the Reported Works with Our Proposal Strategy for Detection of MicroRNA.

Method	Detection range	Detection	References
--------	-----------------	-----------	------------

EC	2 fM-1 nM	2 fM	5
EC	0.02~10.0 pM	8.2 fM	6
ICPMS	0.1-500 fM	41 aM	7
Fluorescence	0-500 fM	3.0 fM	8
ECL	1.0 fM-1.0 nM	0.5 fM	9
ECL	100 aM-100 pM	18.3 aM	This work

Abbreviation: Electrochemical Impedance Spectroscopy (EIS).

References

1. B. Yang, J. C. Xiao, J. I. Wong, J. Guo, Y. C. Wu, L. J. Ong, L. L. Lao, F. Boey, H. Zhang, H. Y. Yang, and Q. C. Zhang, *J. Phys. Chem.*, 2011, **115**, 7924–7927.
2. M. Bardhan, B. Satpati, T. Ghosh and D. Senapati, *J. Mater. Chem. C.*, 2014, **2**, 3795–3804.
3. Q. Wang, Y. Li, B. Liu, Q. Dong, G. Xu, L. Zhang, J. Zhang, *J. Mater. Chem. A.*, 2015, **3** 139-147.
4. M. H. Jiang, S. K. Li, X. Zhong, W. B. Liang, Y. Q. Chai, Y. Zhuo, and R. Yuan, *Anal. Chem.*, 2019, **91**, 3710-3716.
5. C. S. Fang, K. S. Kim, B. Yu, S. Jon, M. S. Kim, and H. Yang, *Anal. Chem.*, 2017, **89**, 2024–2031.
6. J. Wang, S. H. Li, J. G. Xu, Y. S. Lu, M. Lin, C. H. Wang, C. Zhang, G. X. Lin and L. Jia, *Chem. Commun.*, 2020, **56**, 1681.
7. X. Liu, S. Q. Zhang, Z. H. Cheng, X. Wei, T. Yang, Y. L. Yu, M. L. Chen, and J. H. Wang, *Anal. Chem.* 2018, **90**, 12116-12122.
8. C. Y. Li, D. Cao, C. Y. Song, C. M. Xu, X. Y. Ma, Z. L. Zhang, D. W. Pang and H. W. Tang, *Chem. Commun.*, 2017, **53**, 4092.
9. Q. M. Feng, Y. Z. Shen, M. X. Li, Z. L. Zhang, W. Zhao, J. J. Xu, and H. Y. Chen, *Anal. Chem.* 2016, **88**, 937-944.